

MOL # 14019

Involvement of BCRP (ABCG2) in the biliary excretion of pitavastatin

MASARU HIRANO, KAZUYA MAEDA, SOICHIRO MATSUSHIMA, YOSHITANE

NOZAKI, HIROYUKI KUSUHARA, and YUICHI SUGIYAMA

Graduate School of Pharmaceutical Sciences, The University of Tokyo, Tokyo,

Japan

Running title: BCRP-mediated efflux transport of pitavastatin

Corresponding Author:

Yuichi Sugiyama, Ph. D.

Department of Molecular Pharmacokinetics

Graduate School of Pharmaceutical Sciences

The University of Tokyo

7-3-1 Hongo, Bunkyo-ku, Tokyo

113-0033 JAPAN

Phone: +81-3-5841-4770

Fax: +81-3-5841-4766

E-mail: sugiyama@mol.f.u-tokyo.ac.jp

Number of Text Pages: 49

Tables: 3

Figures: 6

References: 40

MOL # 14019

The Number of Words: Abstract: 246

 Introduction: 707

 Discussion: 1258

Abbreviations:

OATP (Oatp), organic anion transporting polypeptide

BCRP (Bcrp); breast cancer resistance protein

BSEP (Bsep), bile salt export pump

MDR (Mdr); multidrug resistance protein

MRP (Mrp), multidrug resistance-associated protein

HEK, human embryonic kidney

MDCK; Madin-Darby canine kidney

HMG-CoA, 3-hydroxy-3-methylglutaryl-coenzyme A

MOI; multiplicity of infection

K_m ; Michaelis constant

V_{max} ; maximum transport velocity

K_i ; inhibition constant

E₂17 β G; 17 β -estradiol-17 β -D-glucuronide

EHBR; Eisai hyperbiliruminemic rat

LC/MS; high-performance liquid chromatography/mass spectrometry

GFP; green fluorescent protein

SNP; single nucleotide polymorphism

Abstract

Pitavastatin, a novel potent HMG-CoA reductase inhibitor, is selectively distributed to the liver and excreted into bile in unchanged form in rats. We previously reported that the hepatic uptake is mainly mediated by OATP1B1, whereas the biliary excretion mechanism remains to be clarified. In the present study, we investigated the role of breast cancer resistance protein (BCRP) in the biliary excretion of pitavastatin. The ATP-dependent uptake of pitavastatin by human and mouse BCRP-expressing membrane vesicles was significantly higher compared with that by control vesicles with K_m values of 5.73 μM and 4.77 μM , respectively. The biliary excretion clearance of pitavastatin in Bcrp1 (-/-) mice was decreased to one-tenth of that in control mice. The biliary excretion of pitavastatin unchanged between control and Eisai hyperbiliruminemic rats (EHBRs), indicating minor contribution of Mrp2. This observation differs radically from that for a more hydrophilic statin, pravastatin of which biliary excretion is largely mediated by Mrp2. These data suggest that the biliary clearance of pitavastatin can be largely accounted for by BCRP in mice. In the case of humans, transcellular transport of pitavastatin was determined in the MDCK II cells expressing OATP1B1, and human canalicular

efflux transporters. A significant basal-to-apical transport of pitavastatin was observed in OATP1B1/MDR1 and OATP1B1/MRP2 double transfectants as well as OATP1B1/BCRP double transfectants, implying the involvement of multiple transporters in the biliary excretion of pitavastatin in humans. This is in contrast to a previous belief that the biliary excretion of statins is mediated mainly by MRP2.

Introduction

The liver plays an important role in the excretion of xenobiotics including many kinds of drugs. A number of reports have shown that several kinds of transporters are expressed on the canalicular membrane in the liver for the efficient elimination of drugs via the bile (Chandra and Brouwer, 2004). It has been generally accepted that transport of various organic anions across the canalicular membrane is mainly mediated by multidrug resistance-associated protein 2 (MRP2/ABCC2), while the bile salt export pump (BSEP/ABCB1) exclusively accepts bile acids and multidrug resistance protein (P-glycoprotein, MDR1/ABCB1) can transport relatively hydrophobic neutral or cationic compounds (Chandra and Brouwer, 2004). However, several reports have shown that some anionic drugs can also be recognized by BSEP and MDR1 (Cvetkovic et al., 1999, Hirano et al, 2005), suggesting that multiple transport mechanisms are involved in the biliary excretion of organic anions.

Moreover, breast cancer resistance protein (BCRP/ABCG2) has been recently cloned and can accept various kinds of organic anions, especially sulfated conjugates of steroids and xenobiotics (Allikmets et al., 1998; Suzuki et al., 2003). Because BCRP is expressed on the bile canalicular membrane of

hepatocytes as well as the brush-border membrane of enterocytes, trophoblast cells in placenta and the apical membrane of lactiferous ducts in the mammary gland (Maliepaard et al., 2001), BCRP must be also considered as one of the routes for the biliary excretion of organic anions. Current evidence indicates that BCRP contributes to the membrane transport of some substrates, such as intestinal absorption and transfer to breast milk (Adachi et al., 2004; Jonker et al., 2002; Jonker et al., 2000; Kondo et al., 2005; Mizuno et al., 2004, Merino et al., 2005a). Regarding the involvement of BCRP in biliary excretion, some reports have demonstrated that the biliary excretion of 2-amino-1-methyl-6-phenylimidazo (4,5-b) pyridine (PhIP) and nitrofurantoin is almost impaired in *Bcrp1* (-/-) mice (Merino et al., 2005a; van Herwaarden et al., 2003) and that the biliary excretion of topotecan and cimetidine is also mainly regulated by *Bcrp*, considering the gender difference in the hepatic expression level of *Bcrp* and the plasma concentration profiles (Merino et al., 2005b). In addition, it has been demonstrated that certain kinds of single nucleotide polymorphisms (SNPs) in BCRP and inhibition of BCRP-mediated transport by some compounds may alter its function and the pharmacokinetics of some drugs *in vitro* (Imai et al., 2002; Kondo et al., 2004; Zamber et al., 2003) as well

as *in vivo* (Kruijtzter et al., 2002; Sparreboom et al., 2004). Therefore, the pharmacokinetics of several important compounds are mainly regulated by BCRP.

Pitavastatin is a highly potent inhibitor of 3-hydroxymethylglutaryl coenzyme A (HMG-CoA) reductase, the rate-limiting enzyme in cholesterol biosynthesis (Kajinami et al., 2003). Pitavastatin causes a significant reduction in not only serum total cholesterol and low-density lipoprotein cholesterol but also triglyceride levels (Stein et al, 1998). It has been demonstrated that [¹⁴C]-pitavastatin is selectively distributed to the liver in rats with a liver-to-plasma concentration ratio of more than 50 (Kimata et al, 1998). We previously demonstrated that pitavastatin is taken up into human hepatocytes mainly by OATP1B1 (OATP2/OATP-C) (Hirano et al., 2004). Then, because it is scarcely metabolized in human liver microsomes (Fujino et al., 2003), pitavastatin is supposed to be excreted into bile in unchanged form (Kojima et al, 2001). However, the biliary transport mechanism of pitavastatin has not been clarified yet. So far, Fujino et al. (2002) have demonstrated that after i.v. bolus administration of pitavastatin, its plasma concentration and biliary excretion in EHBR, an Mrp2-deficient rat, are comparable with those in Sprague-Dawley rats

and that the plasma and brain concentrations of pitavastatin in *mdr1a/1b* knockout mice are not different from those in control mice. Also, we have already shown that pitavastatin is not a substrate of rat and human BSEP (Hirano et al., 2005). These results suggest that BSEP, MRP2 and MDR1 do not make a major contribution to the biliary excretion of pitavastatin.

In the present study, to demonstrate the involvement of BCRP in the biliary excretion of pitavastatin, we examined the transport of pitavastatin by transporter expression systems and observed the biliary excretion clearance of pitavastatin in transporter-deficient animals. Moreover, to check whether other statins could be substrates of BCRP or not, we performed a transport study using BCRP-expressing membrane vesicles.

Materials and Methods

Animals Male Bcrp1 (-/-) and wild-type FVB mice (16-18 weeks old) were used in the present study (Jonker et al., 2002). Male Sprague-Dawley rats (7-8 weeks old) and Eisai hyperbilirubinemic rats (EHBR, 7-8 weeks old) were purchased from SLC (Shizuoka, Japan). All animals were maintained under standard conditions with a reverse dark-light cycle and were treated humanely. Food and water were available *ad libitum*. The studies reported in this manuscript were carried out in accordance with the guidelines provided by the Institutional Animal Care Committee (Graduate School of Pharmaceutical Sciences, the University of Tokyo).

Materials Pitavastatin, monocalcium bis [(3R,5S,6E)-7-[2-cyclopropyl-4-(4-fluorophenyl)-3-quinolyl] 3,5-dihydroxy-6-heptanoate] was synthesized by Nissan Chemical Industries (Chiba, Japan). [³H]-pitavastatin (16.0 Ci/mmol) and [³H]-cerivastatin (4.86 Ci/mmol) were synthesized by Amersham Biosciences (Little Chalfort, UK) and Hartmann Analytic GmbH (Braunschweig, Germany), respectively. [³H]-pravastatin (44.6 Ci/mmol), [¹⁴C]-fluvastatin (45.7 mCi/mmol) and [³H]-rosuvastatin (79 Ci/mmol) were supplied by Sankyo Co., Ltd. (Tokyo, Japan), Novartis Pharma K.K. (Basle,

Switzerland), and AstraZeneca PLC (London, UK), respectively. Other unlabeled HMG-CoA reductase inhibitors (atorvastatin, cerivastatin, fluvastatin, pravastatin, rosuvastatin and simvastatin acid) were donated by Kowa Co., Ltd. (Tokyo, Japan). [³H]-17 β -estradiol-17 β -D-glucuronide (E₂17 β G) and [³H]-estrone-3-sulfate (45 Ci/mmol and 46 Ci/mmol, respectively) were purchased from New England Nuclear (Boston, MA). Unlabeled E₂17 β G and estrone-3-sulfate were purchased from Sigma (St. Louis, MO). All other chemicals were of analytical grade and commercially available.

Cell Culture Human BCRP-, mouse Bcrp- or green fluorescent protein (GFP)-transfected HEK293 cells (Kondo et al., 2004) and MDCKII single- and double-transfected cells expressing human OATP1B1, MDR1, MRP2 or BCRP (Matsushima et al., 2005) and rat Oatp1b2 or Mrp2 (Sasaki et al., 2004) were grown in Dulbecco's modified Eagle's medium (DMEM) low glucose (Invitrogen, Carlsbad, CA) supplemented with 10 % fetal bovine serum (Sigma, St. Louis, MO), 100 U/mL penicillin and 100 μ g/mL streptomycin at 37°C with 5 % CO₂ and 95 % humidity.

Construction and infection of recombinant adenovirus and the membrane

vesicle preparation Details of the procedure for producing recombinant

adenovirus containing human BCRP, mouse Bcrp and GFP have been described previously (Kondo et al., 2004). Membrane vesicles were prepared from BCRP and GFP-transfected HEK293 cells according to the method described (Kondo et al., 2004). For the preparation of the isolated membrane vesicles, HEK293 cells cultured in a 15-cm dish were infected by recombinant adenovirus containing human and mouse BCRP (10 MOI). As a negative control, cells were infected with GFP (10 MOI). Cells were harvested at 48 h after infection, and then the membrane vesicles were isolated from $1\sim 2 \times 10^8$ cells using a standard method described previously in detail (Muller et al., 1994). Briefly, cells were diluted 40-fold with hypotonic buffer (1 mM Tris-HCl, 0.1 mM EDTA, pH 7.4, at 37 °C) and stirred gently for 1 h on ice in the presence of 2 mM phenylmethylsulfonyl fluoride, 5 µg/mL leupeptin, 1 µg/mL pepstatin and 5 µg/mL aprotinin. The cell lysate was centrifuged at 100,000g for 30 min at 4 °C, and the resulting pellet was suspended in 10 mL isotonic TS buffer (10 mM Tris-HCl, 250 mM sucrose, pH 7.4 at 4 °C) and homogenized using a Dounce B homogenizer (glass/glass, tight pestle, 30 strokes). The crude membrane fraction was layered on top of 38 % (w/v) sucrose solution in 5 mM Tris-HEPES, pH 7.4 at 4 °C, and centrifuged in Beckman SW41 rotor

centrifuged at 280,000g for 60 min at 4 °C. The turbid layer at the interface was collected, diluted to 23 mL with TS buffer, and centrifuged at 100,000g for 30 min at 4 °C. The resulting pellet was suspended in 400 µL TS buffer. Vesicles were formed by passing the suspension 30 times through a 27-gauge needle using a syringe. The membrane vesicles were finally frozen in liquid nitrogen and stored at -80 °C until use. Protein concentrations were determined by the Lowry method and bovine serum albumin was used as a standard.

Transport Studies with Membrane Vesicles The transport studies were performed using a rapid filtration technique (Hirohashi et al., 1999). Briefly, 15 µL transport medium (10 mM Tris-HCl, 250 mM sucrose, 10 mM MgCl₂, pH 7.4) containing radiolabeled compounds, with or without unlabeled substrate, was preincubated at 37 °C for 3 min and then rapidly mixed with 5 µL membrane vesicle suspension (5 µg protein). The reaction mixture contained 5 mM ATP or AMP, along with the ATP-regenerating system (10 mM creatine phosphate and 100 µg/µL creatine phosphokinase). The transport reaction was terminated by the addition of 1 mL ice-cold buffer containing 10 mM Tris-HCl, 250 mM sucrose and 0.1 M NaCl (pH 7.4). The stopped reaction mixture was

filtered through a 0.45- μm HA filter (Millipore Corp., Bedford, MA) and then washed twice with 5 mL stop solution. Radioactivity retained on the filter was determined in a liquid scintillation counter (LS6000SE, Beckman Instruments, Fullerton, CA, USA) after the addition of scintillation cocktail (Clear-sol I, Nacalai Tesque, Tokyo, Japan).

Transcellular Transport Study Transfected MDCK II cells were seeded in 24-well plates at a density of 1.4×10^5 cells per well and cultured with 10 mM sodium butyrate for 24 h prior to the transport study (Sasaki et al., 2002). Krebs-Henseleit buffer consisted of 142 mM NaCl, 23.8 mM Na_2CO_3 , 4.83 mM KCl, 0.96 mM KH_2PO_4 , 1.20 mM MgSO_4 , 12.5 mM HEPES, 5 mM glucose, and 1.53 mM CaCl_2 adjusted to pH 7.4. The experiments were initiated by replacing the medium on either the apical or basal side of the cell layer with complete medium containing tritium labeled and unlabeled E_2 or pitavastatin (0.1 μM). The cells were incubated at 37 °C, and aliquots of medium were taken from each compartment at designated time points. Radioactivity in 100 μL medium was measured in a liquid scintillation counter (LS 6000SE, Beckman Instruments, Inc., Fullerton, CA) after the addition of scintillation cocktail (Clear-sol I, Nacalai Tesque, Tokyo, Japan). At the end of

the experiments, the cells were washed three times with 1.5 mL ice-cold Krebs-Henseleit buffer and solubilized in 450 μ L 0.2 N NaOH. After addition of 225 μ L 0.4 N HCl, 600 μ L aliquots were transferred to scintillation vials. 50 μ L aliquots of cell lysate were used to determine protein concentrations as described above.

Kinetic Analysis Ligand uptake was normalized in terms of the amount of membrane protein and expressed as the uptake volume [μ L/mg protein], given as the amount of radioactivity associated with the cells [dpm/mg protein] divided by its concentration in the incubation medium [dpm/ μ L]. The ATP-dependent uptake of ligands via BCRP was calculated by subtracting the ligand in the presence of AMP from that in the presence of ATP. Kinetic parameters were obtained using the following equation:

$$v = \frac{V_{\max} \times S}{K_m + S} \quad (\text{Eq. 1})$$

, where v is the uptake velocity of the substrate (pmol/min/mg protein), S is the substrate concentration in the medium (μ M), K_m is the Michaelis constant (μ M), and V_{\max} is the maximum uptake velocity (pmol/min/mg protein). The Damping Gauss Newton Method algorithm was used with a MULTI program

(Yamaoka et al, 1981) to perform non-linear least-squares data fitting. Inhibition constants (K_i) of a series of compounds were calculated by the following equation, if the substrate concentration was much lower than the K_m value.

$$CL(+I) = \frac{CL}{(1 + I / K_i)} \quad (\text{Eq. 2})$$

, where CL represents the uptake clearance in the absence of inhibitor, $CL(+I)$ represents the uptake clearance in the presence of inhibitor and I represents the concentration of inhibitor. When fitting the data to determine the K_i value, the input data were weighed as the reciprocal of the observed values.

***In vivo* infusion study in rats** Male Sprague-Dawley rats and EHBR

weighing approximately 250 to 300 g were used for these experiments. Under pentobarbital anesthesia (30 mg/kg), the femoral vein was cannulated with a polyethylene catheter (PE-50) for the injection of [^3H]-pitavastatin. The bile duct was cannulated with a polyethylene catheter (PE-10) for bile collection. The rats received a constant infusion of pitavastatin at a dose of 72 $\mu\text{g}/\text{h}/\text{kg}$ following a bolus i.v. administration of 0.25 mg/kg. Blood samples were collected from the jugular vein. Bile was collected in preweighed test-tubes at

30-min intervals throughout the experiment. Plasma was prepared by centrifugation of the blood samples (10,000g; Microfuge, Beckman, Fullerton, CA). The rats were killed after 210 min, and the entire liver was excised immediately. Then the liver was weighed and minced, and subsequently 200 μ L hydroxyperoxide and 400 μ L isopropanol were added to approximately 200 mg liver. This was incubated at 55 °C for 4-6 h after the addition of 2 mL solouene (PerkinElmer Life and Analytical Sciences, Boston, MA) to dissolve the tissues, and then the radioactivity was determined in a liquid scintillation counter after the addition of scintillation cocktail.

***In vivo* infusion study in mice and quantification of pitavastatin by LC/MS**

Male FVB and Bcrp1 (-/-) mice weighing approximately 28 to 33 g were used throughout these experiments. Under pentobarbital anesthesia (30 mg/kg), the jugular vein was cannulated with a polyethylene catheter (PE-10) for the injection of pitavastatin. The bile duct was cannulated with a polyethylene catheter (SP-8) for bile collection. The mice received a constant infusion of pitavastatin at a dose of 300 μ g/h/kg. Blood samples were collected from the opposite jugular vein. Bile was collected in preweighed test-tubes at 15-min intervals throughout the experiments. Plasma was prepared by centrifugation

of the blood samples. The mice were killed after 150 min, and the entire liver, kidney, brain and skeletal muscle were excised immediately. The tissues were weighed and stored at -80°C until quantification. Portions of liver, kidney, brain and skeletal muscle were added to five volumes of physiological saline (w/v) and homogenized. Plasma (10 µL), bile (1 µL), or tissue homogenate (10 or 100 µL) was deproteinized with 200 µL methanol containing the internal standard (atorvastatin, 40 ng/mL), followed by centrifugation at 4 °C and 10,000g for 10 min. The supernatant (100 µL) was mixed with 50 µL water and subjected to HPLC (Waters 2695, Waters, Milford, MA). The LC/MS analysis of pitavastatin was performed using an Inertsil ODS-3 column (50 × 2.1 mm, particle size 5 µm) (GL Sciences, Tokyo, Japan). The mobile phase consisted of methanol:ammonium formate buffer (pH 4) =7:3 (v/v) and the flow rate was 0.7 mL/min. The MS instrument used for this work was a ZQ micromass (Waters, Milford, MA) equipped with a Z-spray source and operated in the positive-ion electrospray ionization mode. The Z-spray desolvation temperature, capillary voltage and cone voltage were 350 °C, 3400 V and 40 V, respectively. The m/z monitored for pitavastatin and atorvastatin was 422.3 and 559.0, respectively. No chromatographic interference was found for

pitavastatin and atorvastatin in extracts from blank plasma, bile, and tissue homogenates. The retention times of pitavastatin and atorvastatin were 1.2 and 1.1 min, respectively. The detection limits for pitavastatin were 5, 2000, 100, 5, 5 and 5 ng/mL in plasma, bile, liver, kidney, brain and muscle, respectively.

Pharmacokinetic Analysis Total plasma clearance (CL_{total}), biliary clearance normalized by circulating plasma ($CL_{bile,plasma}$), and biliary clearance normalized by the liver concentration ($CL_{bile,liver}$) were calculated from the following equations:

$$CL_{total} = I/C_{ss,plasma} \quad (\text{Eq. 3})$$

$$CL_{bile,plasma} = V_{bile}/C_{ss,plasma} \quad (\text{Eq. 4})$$

$$CL_{bile,liver} = V_{bile}/C_{ss,liver} \quad (\text{Eq. 5})$$

where I , $C_{ss,plasma}$, V_{bile} , and, $C_{ss,liver}$ represent the infusion rate ($\mu\text{g}/\text{min}/\text{kg}$), plasma concentrations at steady-state (ng/mL), biliary excretion rate at steady-state ($\mu\text{g}/\text{min}/\text{kg}$), and hepatic concentration at steady-state (ng/mL), respectively. In rats, $C_{ss,plasma}$ was determined as the mean value of the plasma [^3H]-pitavastatin concentrations at 60, 90, 120, 150, 180 and 210 min.

V_{bile} was determined as the mean value of the biliary excretion rate of [^3H]-pitavastatin from 60 to 90 min, from 90 to 120 min, from 120 to 150 min, from 150 to 180 min, and from 180 to 210 min. In mice, $C_{\text{ss,plasma}}$ was determined as the mean value of the plasma unlabeled pitavastatin concentrations at 90, 120 and 150 min. V_{bile} was determined as the mean value of the biliary excretion rate of unlabeled pitavastatin from 90 to 105 min, from 105 to 120 min, from 120 to 135 min, and from 135 to 150 min. $C_{\text{ss,liver}}$ was determined as the hepatic pitavastatin concentration at the end of the *in vivo* experiment. To calculate $C_{\text{ss,liver}}$, the specific gravity of the liver was assumed to be unity. Thus, the amount in the liver (ng/g liver) can be regarded as the hepatic concentration (ng/g), and the units of $\text{CL}_{\text{bile,liver}}$ should be milliliters per minute per kilogram.

Statistical Analysis Statistically significant differences were determined using one-way analysis of variance followed by Fisher's least significant difference method. Differences were considered to be significant at $P < 0.05$.

Results

ATP-dependent uptake of [³H]-pitavastatin into BCRP-expressing

membrane vesicles

The time profiles and Eadie-Hofstee plots for the uptake of [³H]-pitavastatin by BCRP-expressing membrane vesicles are shown in Fig. 1.

The uptake of [³H]-pitavastatin into membrane vesicles from human and mouse BCRP-transfected HEK293 cells was markedly stimulated by ATP, but not that

into GFP-transfected control cells (Fig. 1A and 1B). The

concentration-dependence of human and mouse BCRP-mediated

ATP-dependent uptake of pitavastatin is shown in Fig. 1C and 1D. The K_m and

V_{max} values for the ATP-dependent uptake of pitavastatin were $5.73 \pm 1.52 \mu\text{M}$

and $1106 \pm 79 \text{ pmol/min/mg protein}$ by human BCRP, $4.77 \pm 0.50 \mu\text{M}$ and $881 \pm$

$20 \text{ pmol/min/mg protein}$ by mouse Bcrp, respectively.

Uptake of other statins into BCRP-expressing membrane vesicles

Uptake of other statins into human and mouse BCRP-expressing membrane vesicles

was observed (Fig. 2). We did not see any significant ATP-dependent uptake

of cerivastatin and fluvastatin by mouse Bcrp-expressing membrane vesicles

compared with GFP-transfected vesicles, while human BCRP significantly

recognized all the statins we tested (cerivastatin, fluvastatin, pitavastatin, pravastatin and rosuvastatin) as a substrate (Fig. 2 A-E). Estrone-3-sulfate (0.1 μ M), which was a positive control compound for BCRP-mediated transport, was accepted as a substrate of both human and mouse BCRP (Fig. 2F). The K_m value of estrone-3-sulfate by mouse Bcrp was $16.4 \pm 3.0 \mu$ M (data not shown).

Inhibitory effects of statins on the ATP-dependent uptake of [³H]-estrone-3-sulfate into human and mouse BCRP-expressing membrane vesicles

The inhibitory effects of statins on the ATP-dependent uptake of [³H]-estrone-3-sulfate by human and mouse BCRP-expressing membrane vesicles were observed. All the statins, except for pravastatin ($\sim 300 \mu$ M), inhibited the ATP-dependent uptake of [³H]-estrone-3-sulfate by human and mouse BCRP in a dose-dependent manner. The K_i values of statins for human and mouse BCRP are summarized in Table 1.

Transcellular transport of pitavastatin across double transfectants

Transcellular transport of pitavastatin across double-transfected MDCK II

monolayers expressing uptake transporter (OATP1B1) and efflux transporter (MDR1, MRP2 or BCRP) was compared with that across the single-transfected monolayer and the vector-transfected control monolayer. In the case of humans, as shown in Fig. 3, a symmetrical flux of pitavastatin was observed across the control, MDR1-, MRP2- and BCRP-expressing MDCK II monolayer. The basal-to-apical flux of pitavastatin across the OATP1B1-expressing monolayer was approximately twice that in the opposite direction, whereas the basal-to-apical flux of pitavastatin was approximately 15, 110 and 230 times higher than that in the opposite direction in OATP1B1/MRP2, OATP1B1/BCRP and OATP1B1/MDR1 double transfected cells, respectively. In addition, transcellular transport of pitavastatin across double-transfected MDCK II monolayers expressing rat Oatp1b2 and Mrp2 was also compared with that across the Oatp1b2 or Mrp2 single-transfected monolayer and the vector-transfected control monolayer. The basal-to-apical flux of pitavastatin was 2.4 times higher than that in the opposite direction in the Oatp1b2/Mrp2 double-transfected cells, though a smaller vectorial transport was observed even in the Oatp1b2 expressing monolayer (Fig. 4). In both rats and humans, we checked the transcellular transport of E₂17 β G as a positive control in parallel

and obtained similar results to those measured previously (data not shown, Matsushima et al, 2005).

Plasma, liver concentration and biliary excretion profiles at steady-state in

Sprague-Dawley rats and EHBR It has been reported that pitavastatin is not significantly metabolized in rats and over 70% of the intact form can be detected in bile (Fujino et al., 2002). Therefore, we used [³H]-labeled pitavastatin in rats in an *in vivo* study to examine the involvement of Mrp2 in the biliary excretion of pitavastatin. The plasma concentration of pitavastatin reached a plateau at 60 min during constant infusion following a bolus i.v. administration. The biliary excretion rate (V_{bile}), the steady-state plasma concentration ($C_{\text{ss,plasma}}$), and total clearance (CL_{total}) values of pitavastatin in EHBR were almost the same as those in normal rats (Fig. 5 and Table 2). The concentration of pitavastatin and the K_p value in the liver at steady-state in EHBR were lower than those in normal rats, and the $CL_{\text{bile,plasma}}$ and $CL_{\text{bile,liver}}$ in EHBR were slightly higher than those in normal rats, although the differences were not statistically significant (Fig. 5).

Plasma, tissue concentration and biliary excretion profiles at steady-state in FVB and Bcrp1 (-/-) mice The plasma concentration of pitavastatin reached a plateau at 90 min during constant infusion (Fig. 6). The V_{bile} of parent pitavastatin in Bcrp1 (-/-) mice was much lower than that in control mice, while the $C_{ss,plasma}$ and CL_{total} of pitavastatin in Bcrp1 (-/-) mice did not differ from those in normal mice (Table 3). The K_p values of pitavastatin in the kidney, brain and skeletal muscle as well as the liver (Table 3) at steady-state were similar in control and Bcrp1 (-/-) mice (K_p value for kidney 1.41 ± 0.10 and 1.48 ± 0.12 ng/g, for brain 0.0308 ± 0.0027 and 0.0322 ± 0.0070 ng/g, and for skeletal muscle 0.0985 ± 0.0075 and 0.0960 ± 0.0061 ng/g in wild type and Bcrp1 (-/-) mice, respectively).

Discussion

Pitavastatin, a new potent inhibitor of HMG-CoA reductase, is scarcely metabolized in humans and is thought to be excreted into the bile in intact form. In the present study, we concentrated on a new candidate transporter, BCRP, for the biliary excretion of pitavastatin.

ATP-dependent uptake of pitavastatin in human and mouse BCRP-expressing membrane vesicles was observed (Fig. 1). The K_m value of pitavastatin for human BCRP (5.73 μM) was almost the same as that for mouse Bcrp (4.77 μM) and these K_m values were similar to that of estrone-3-sulfate, which is a well-known substrate of human BCRP (Suzuki et al., 2003), indicating that pitavastatin is also a good substrate of BCRP. Regarding other statins, as shown in Table 1, no species difference in the K_i value of each statin for the BCRP-mediated uptake of estrone-3-sulfate was observed between humans and mice. The inhibition potency of statins, except pravastatin, was almost identical, whereas pravastatin could not inhibit the BCRP-mediated transport of estrone-3-sulfate up to 300 μM . On the other hand, all statins we tested could be substrates of human BCRP, whereas four of them were also substrates of mouse Bcrp (Fig. 2). From a pharmacokinetic viewpoint, BCRP

could at least partly contribute to the biliary excretion of pravastatin, pitavastatin and rosuvastatin, which are scarcely metabolized by metabolic enzymes like cytochrome P450 in the liver. On the other hand, in the case of atorvastatin, cerivastatin and simvastatin, which have been reported to be extensively metabolized by P450 enzymes (Garcia et al., 2003), implying that the biliary excretion of their unchanged form via BCRP was considered to be minor in *in vivo* situations.

To estimate the contribution of each transporter to the biliary excretion of pitavastatin in the *in vivo* study, the biliary excretion of pitavastatin at steady-state was investigated using Mrp2- and Bcrp1-deficient animals. Since pitavastatin was found to be scarcely metabolized in rats (Fujino et al, 2002), the radioactivity would reflect the parent pitavastatin. We confirmed that the plasma concentration and biliary excretion rate of pitavastatin was not changed between Sprague-Dawley rat and EHBR (Fig. 5, Table. 2), which is consistent with a previous report (Fujino et al., 2002). Therefore, the involvement of Mrp2 in the biliary excretion of pitavastatin is minor. The liver concentration in EHBR was significantly lower than that in control rats possibly because of i) the accelerated efflux via the basolateral membrane in the liver caused by the

induction of Mrp3 (Ogawa et al., 2000) and ii) the inhibition of hepatic uptake process from the blood by a higher concentration of bilirubin glucuronide in EHBR (Sathirakul et al., 1993) or by the decrease in the expression levels of transporters responsible for the uptake of pitavastatin.

Biliary excretion of pitavastatin was also observed in Bcrp1 (-/-) and control mice. In contrast to humans and rats, pitavastatin is extensively metabolized in mice and so we decided to quantify the unchanged form separately by LC/MS in mice. The biliary excretion clearance of pitavastatin in Bcrp1 (-/-) mice was ten times lower than that in control mice, suggesting that unchanged pitavastatin is excreted into bile mainly by Bcrp. In control mice, the biliary clearance normalized by plasma concentration ($CL_{\text{bile,plasma}}$) accounted for only 5 % of the plasma total clearance (CL_{total}), indicating that pitavastatin is mainly excreted into bile as metabolites. Taking extensive metabolism into consideration, it is natural that the plasma and liver concentrations were not different between Bcrp1 (-/-) and control mice, even if the biliary clearance of the parent compound was drastically reduced in Bcrp1 (-/-) mice. In contrast to mice, pitavastatin is thought to be excreted into the bile in an intact form with only minimal metabolism in humans (Fujino et al., 2003). Therefore, BCRP is

estimated to be involved in the biliary excretion of pitavastatin in humans. On the other hand, a previous *in vivo* study using EHBR revealed that Mrp2 is a major transporter for the excretion of pravastatin in rats (Yamazaki et al, 1997). Even although pitavastatin and pravastatin belong to the same category, HMG-CoA reductase inhibitors, it was interesting to find that pitavastatin and pravastatin are excreted into the bile by different efflux transport systems. In the brain and kidney, in which BCRP is also expressed, and skeletal muscle, which is a target site of severe adverse effects of statins (rhabdomyolysis), these tissue concentrations were not significantly different between Bcrp1 (-/-) and control mice. Thus, Bcrp does not contribute to the distribution of pitavastatin in these tissues. BCRP was expressed not only in the liver, kidney and brain but also small intestine and mammary gland (Doyle and Ross, 2003). Recently, it was demonstrated that BCRP critically modulates the absorption of certain drugs from the small intestine and transfer to milk (Adachi et al, 2004; Merino et al, 2005a). Further studies are needed to clarify the importance of BCRP in the intestinal absorption and tissue distribution of a series of statins.

In Fig. 3, we clearly observed the vectorial basal-to-apical transport of pitavastatin across all the double transfectants (OATP1B1/BCRP,

OATP1B1/MDR1 and OATP1B1/MRP2) in contrast to that across the control and OATP1B1-single transfected cells. The efflux transport clearance of pitavastatin normalized by the intracellular concentration did not differ much among MDR1, MRP2 and BCRP, the range being only two-fold. In the case of pravastatin, we previously demonstrated that the efflux clearance of MRP2 was much higher than that of MDR1 and BCRP (Matsushima et al, 2005).

Considering these facts, the relative contribution of MDR1 and BCRP to the biliary excretion of pitavastatin was larger than that of pravastatin. In the case of rats, the basal-to-apical flux of pitavastatin across the Oatp1b2/Mrp2 double transfectants was significantly higher than that across the Oatp1b2-single transfectants (Fig. 4). However, the ratio of basal-to-apical to apical-to-basal flux of pitavastatin in Oatp1b2/Mrp2 double transfected cells divided by that in Oatp1b2 single transfected cells was approximately 1.6, which was small in comparison with that of other substrates previously tested (Sasaki et al., 2004).

Therefore, although pitavastatin is a substrate of rat Mrp2, the intrinsic efflux clearance of pitavastatin via rat Mrp2 appears to be relatively low.

Recently, the elimination of diflomotecan from plasma was found to be delayed in patients with frequently observed SNP in BCRP (C421A/Q141K)

(Sparreboom et al., 2004). Various reports suggested that this SNP affected the protein expression level of BCRP in the placenta without changing its intrinsic efflux clearance (Kobayashi et al., 2005; Kondo et al., 2004). On the other hand, both *in vivo* and *in vitro* studies revealed that frequently-observed haplotype, OATP1B1*15 (N130D and V174A), reduced the non-renal clearance of pravastatin (Iwai et al., 2004; Nishizato et al., 2003). We previously demonstrated that pitavastatin is taken up into hepatocytes mainly by OATP1B1 (Hirano et al., 2004). Taking these facts into consideration, further clinical studies are needed to investigate the effect of SNPs in OATP1B1 and BCRP on the pharmacokinetics of pitavastatin and to determine the importance of each transporter directly in humans.

In the present study, we have shown that pitavastatin is recognized by human and mouse BCRP in expression systems and Bcrp is mainly involved in the biliary excretion of pitavastatin by knockout animals. BCRP can also accept other statins as a substrate, implying that it is important to estimate how the change of function and expression level of BCRP affects the pharmacokinetics of statins. In humans, because it is evident that pitavastatin is a substrate of BCRP, MDR1 and MRP2 by double transfectants, it will be

important to estimate the contribution of each transporter to the biliary excretion of pitavastatin in humans.

Acknowledgements

We would like to thank Dr. Alfred H Schinkel (The Netherlands Cancer Institute, the Netherlands) and Dr. Johan A Jonker (The Salk Institute for Biological Studies, CA, USA) for constructing Bcrp1 (-/-) mice and giving us valuable comments, Dr. Piet Borst (The Netherlands Cancer Institutes) for providing the MDCKII cells expressing MRP2 and MDR1 and Dr. Yoshihiro Miwa (Univ. Tsukuba, Japan) for providing pEB6CAGMCS/SRZeo vector. We would also like to thank Dr. Makoto Sasaki for constructing Oatp1b2/Mrp2 double transfected cells and Ms. Chihiro Kondo for constructing human BCRP-recombinant adenovirus. We also thank Sankyo Co., Ltd. (Tokyo, Japan) for providing radiolabeled pravastatin, Novartis Pharma K.K. (Basle, Switzerland) for providing radiolabeled fluvastatin, AstraZeneca PLC (London, UK) for providing radiolabeled rosuvastatin and Kowa Co. Ltd. (Tokyo, Japan) for providing radiolabeled pitavastatin and unlabeled statins.

References

- Adachi Y, Suzuki H, Schinkel AH and Sugiyama Y (2004) Role of breast cancer resistance protein (Bcrp1/Abcg2) in the extrusion of glucuronide and sulfate conjugates from enterocytes to intestinal lumen. *Mol Pharmacol* **67**:923-8.
- Allikmets R, Schriml LM, Hutchinson A, Romano-Spica V and Dean M (1998) A human placenta-specific ATP-binding cassette gene (ABCP) on chromosome 4q22 that is involved in multidrug resistance. *Cancer Res* **58**:5337-9.
- Chandra P and Brouwer KL (2004) The complexities of hepatic drug transport: current knowledge and emerging concepts. *Pharm Res* **21**:719-35.
- Cvetkovic M, Leake B, Fromm MF, Wilkinson GR and Kim RB (1999) OATP and P-glycoprotein transporters mediate the cellular uptake and excretion of fexofenadine. *Drug Metab Dispos* **27**:866-71.
- Doyle LA and Ross DD (2003) Multidrug resistance mediated by the breast cancer resistance protein BCRP (ABCG2). *Oncogene* **22**:7340-58.

Fujino H, Saito T, Tsunenari Y and Kojima J (2003) Interaction between several medicines and statins. *Arzneimittelforschung* **53**:145-53.

Fujino H, Yamada I, Shimada S and Kojima J (2002) Metabolic Fate of Pitavastatin, a New Inhibitor of HMG-CoA Reductase-Effect of cMOAT Deficiency on Hepatobiliary Excretion in Rats and of *mdr1a/b* Gene Disruption on Tissue Distribution in Mice. *Drug Metab Pharmacokinet* **17**:449-56.

Garcia MJ, Reinoso RF, Sanchez Navarro A and Prous JR (2003) Clinical pharmacokinetics of statins. *Methods Find Exp Clin Pharmacol* **25**:457-81.

Hirano M, Maeda K, Shitara Y and Sugiyama Y (2004) Contribution of OATP2 (OATP1B1) and OATP8 (OATP1B3) to the hepatic uptake of pitavastatin in humans. *J Pharmacol Exp Ther* **311**:139-46.

Hirano M, Maeda K, Hayashi H, Kusuhara H and Sugiyama Y (2005) Bile salt export pump (BSEP/ABCB11) can transport a non-bile acid substrate, pravastatin. *J Pharmacol Exp Ther*, accepted.

Hirohashi T, Suzuki H, Chu XY, Tamai I, Tsuji A and Sugiyama Y (2000)

Function and expression of multidrug resistance-associated protein family in human colon adenocarcinoma cells (Caco-2). *J Pharmacol Exp Ther* **292**:265-70.

Hirohashi T, Suzuki H and Sugiyama Y (1999) Characterization of the transport

properties of cloned rat multidrug resistance-associated protein 3 (MRP3). *J Biol Chem* **274**:15181-5.

Imai Y, Nakane M, Kage K, Tsukahara S, Ishikawa E, Tsuruo T, Miki Y and

Sugimoto Y (2002) C421A polymorphism in the human breast cancer resistance protein gene is associated with low expression of Q141K protein and low-level drug resistance. *Mol Cancer Ther* **1**:611-6.

Iwai M, Suzuki H, Ieiri I, Otsubo K and Sugiyama Y (2004) Functional analysis

of single nucleotide polymorphisms of hepatic organic anion transporter OATP1B1 (OATP-C). *Pharmacogenetics* **14**:749-57.

Jonker JW, Buitelaar M, Wagenaar E, Van Der Valk MA, Scheffer GL, Scheper

RJ, Plosch T, Kuipers F, Elferink RP, Rosing H, Beijnen JH and Schinkel AH (2002) The breast cancer resistance protein protects against a major

chlorophyll-derived dietary phototoxin and protoporphyria. *Proc Natl*

Acad Sci U S A **99**:15649-54.

Jonker JW, Smit JW, Brinkhuis RF, Maliepaard M, Beijnen JH, Schellens JH

and Schinkel AH (2000) Role of breast cancer resistance protein in the

bioavailability and fetal penetration of topotecan. *J Natl Cancer Inst*

92:1651-6.

Kajinami K, Takekoshi N and Saito Y (2003) Pitavastatin: efficacy and safety

profiles of a novel synthetic HMG-CoA reductase inhibitor. *Cardiovasc*

Drug Rev **21**:199-215.

Kimata H, Fujino H, Koide T, Yamada Y, Tsunenari Y, Yonemitsu M, and

Yanagawa Y (1998) Studies on the metabolic fate of NK-104, a new

inhibitor of HMG-CoA reductase: I. Absorption, distribution, metabolism

and excretion in rats. *Xenobio Metabol Dispos* **13**: 484–498.

Kojima J, Ohshima T, Yoneda M, and Sawada H (2001) Effect of biliary

excretion on the pharmacokinetics of pitavastatin (NK-104) in dogs.

Xenobio Metab Disp **16**: 497–502.

Kondo C, Suzuki H, Itoda M, Ozawa S, Sawada J, Kobayashi D, Ieiri I, Mine K, Ohtsubo K and Sugiyama Y (2004) Functional analysis of SNPs variants of BCRP/ABCG2. *Pharm Res* **21**:1895-903.

Kondo C, Onuki R, Kusuhara H, Suzuki H, Suzuki M, Okudaira N, Kojima M, Ishiwata K, Jonker JW and Sugiyama Y (2005) Lack of improvement of oral absorption of ME3277 by prodrug formation is ascribed to the intestinal efflux mediated by breast cancer resistant protein (BCRP/ABCG2). *Pharm Res* **22**:613-8.

Kruijtzter CM, Beijnen JH, Rosing H, ten Bokkel Huinink WW, Schot M, Jewell RC, Paul EM and Schellens JH (2002) Increased oral bioavailability of topotecan in combination with the breast cancer resistance protein and P-glycoprotein inhibitor GF120918. *J Clin Oncol* **20**:2943-50.

Maliepaard M, Scheffer GL, Faneyte IF, van Gastelen MA, Pijnenborg AC, Schinkel AH, van De Vijver MJ, Scheper RJ and Schellens JH (2001) Subcellular localization and distribution of the breast cancer resistance protein transporter in normal human tissues. *Cancer Res* **61**:3458-64.

Matsushima S, Maeda K, Kondo C, Hirano M, Sasaki M, Suzuki H and

Sugiyama Y (2005) Identification of the hepatic efflux transporters of organic anions using double transfected MDCKII cells expressing human OATP1B1/MRP2, OATP1B1/MDR1 and OATP1B1/BCRP. *J Pharmacol Exp Ther*, accepted.

Merino G, Jonker JW, Wagenaar E, van Herwaarden AE and Schinkel AH

(2005a) The Breast Cancer Resistance Protein (BCRP/ABCG2) affects pharmacokinetics, hepatobiliary excretion and milk secretion of the antibiotic nitrofurantoin. *Mol Pharmacol*. **65**:1758-64.

Merino G, van Herwaarden AE, Wagenaar E, Jonker JW and Schinkel AH

(2005b) Sex-dependent expression and activity of the ABC transporter Breast Cancer Resistance Protein (BCRP/ABCG2) in liver. *Mol Pharmacol*. **67**:1765-71.

Mizuno N, Suzuki M, Kusuhara H, Suzuki H, Takeuchi K, Niwa T, Jonker JW

and Sugiyama Y (2004) Impaired renal excretion of 6-hydroxy-5,7-dimethyl-2-methylamino-4-(3-pyridylmethyl) benzothiazole

(E3040) sulfate in breast cancer resistance protein (BCRP1/ABCG2)

knockout mice. *Drug Metab Dispos* **32**:898-901.

Muller M, Meijer C, Zaman GJ, Borst P, Scheper RJ, Mulder NH, de Vries EG

and Jansen PL (1994) Overexpression of the gene encoding the

multidrug resistance-associated protein results in increased

ATP-dependent glutathione S-conjugate transport. *Proc Natl Acad Sci U*

S A **91**:13033-7.

Ogawa K, Suzuki H, Hirohashi T, Ishikawa T, Meier PJ, Hirose K, Akizawa T,

Yoshioka M and Sugiyama Y (2000) Characterization of inducible nature

of MRP3 in rat liver. *Am J Physiol Gastrointest Liver Physiol*

278:G438-446.

Nishizato Y, Ieiri I, Suzuki H, Kimura M, Kawabata K, Hirota T, Takane H, Irie S,

Kusuhara H, Urasaki Y, Urae A, Higuchi S, Otsubo K and Sugiyama Y

(2003) Polymorphisms of OATP-C (SLC21A6) and OAT3 (SLC22A8)

genes: consequences for pravastatin pharmacokinetics. *Clin Pharmacol*

Ther **73**:554-65.

Sasaki M, Suzuki H, Aoki J, Ito K, Meier PJ and Sugiyama Y (2004) Prediction of *in vivo* biliary clearance from the *in vitro* transcellular transport of organic anions across a double-transfected Madin-Darby canine kidney II monolayer expressing both rat organic anion transporting polypeptide 4 and multidrug resistance associated protein 2. *Mol Pharmacol* **66**:450-9.

Sasaki M, Suzuki H, Ito K, Abe T and Sugiyama Y (2002) Transcellular transport of organic anions across a double-transfected Madin-Darby canine kidney II cell monolayer expressing both human organic anion-transporting polypeptide (OATP2/SLC21A6) and Multidrug resistance-associated protein 2 (MRP2/ABCC2). *J Biol Chem* **277**:6497-503.

Sathirakul K, Suzuki H, Yasuda K, Hanano M, Tagaya O, Horie T and Sugiyama Y (1993) Kinetic analysis of hepatobiliary transport of organic anions in Eisai hyperbilirubinemic mutant rats. *J Pharmacol Exp Ther* **265**:1301-1312.

Sparreboom A, Gelderblom H, Marsh S, Ahluwalia R, Obach R, Principe P, Twelves C, Verweij J and McLeod HL (2004) Diflomotecan

pharmacokinetics in relation to ABCG2 421C>A genotype. *Clin*

Pharmacol Ther **76**:38-44.

Stein EA, Lane M, Laskarzewski P (1998) Comparison of statins in

hypertriglyceridemia *Am J Cardiol* **26**;81 66B-89B

Suzuki M, Suzuki H, Sugimoto Y and Sugiyama Y (2003) ABCG2 transports

sulfated conjugates of steroids and xenobiotics. *J Biol Chem*

278:22644-9.

van Herwaarden AE, Jonker JW, Wagenaar E, Brinkhuis RF, Schellens JH,

Beijnen JH and Schinkel AH (2003) The breast cancer resistance protein

(Bcrp1/Abcg2) restricts exposure to the dietary carcinogen

2-amino-1-methyl-6-phenylimidazo[4,5-b]pyridine. *Cancer Res*

63:6447-52.

Yamaoka K, Tanigawara Y, Nakagawa T and Uno T (1981) A pharmacokinetic

analysis program (multi) for microcomputer. *J Pharmacobiodyn* **4**:879-85.

Yamazaki M, Akiyama S, Ni'inuma K, Nishigaki R and Sugiyama Y (1997)

Biliary excretion of pravastatin in rats: contribution of the excretion

pathway mediated by canalicular multispecific organic anion transporter.

Drug Metab Dispos **25**:1123-9.

Zamber CP, Lamba JK, Yasuda K, Farnum J, Thummel K, Schuetz JD and

Schuetz EG (2003) Natural allelic variants of breast cancer resistance

protein (BCRP) and their relationship to BCRP expression in human

intestine. *Pharmacogenetics* **13**:19-28.

Footnotes

This work was supported by a Health and Labour Sciences Research Grants from Ministry of Health, Labour and Welfare for the Research on Advanced Medical Technology.

Legends to figures

Fig. 1 Time-profiles and Eadie-Hofstee plots of the uptake of [³H]-pitavastatin by human and mouse BCRP-expressing membrane vesicles. The uptake of 0.1 μM [³H]-pitavastatin by human BCRP (hBCRP) (A) and mouse Bcrp (mBcrp) (B), respectively, was examined at 37 °C in medium containing 5 mM ATP (closed symbols) or AMP (open symbols). Circles and triangles represent the uptake in hBCRP- (or mBcrp-) and GFP-expressing membrane vesicles, respectively. The hBCRP- (C) and mBcrp- (D) mediated uptake of [³H]-pitavastatin was determined for 2 and 1 min, respectively. Each point represents the mean ± S.E. (n = 3). Where vertical bars are not shown, the S.E. values are within the limits of the symbols. The data were fitted to the Michaelis-Menten equation by nonlinear regression analysis, as described under **Materials and Methods**, and each solid line represents the fitted curve.

Fig. 2 The ATP-dependent uptake of statins by human BCRP (hBCRP)-, mouse Bcrp (mBcrp)- and GFP-expressing membrane vesicles. The uptake of 0.1 μM [³H]-cerivastatin (A), 5 μM [¹⁴C]-fluvastatin (B), 0.1 μM [³H]-pitavastatin (C), 0.1 μM [³H]-pravastatin (D) and 0.1 μM [³H]-rosuvastatin (E) for 5 min and

0.1 μM [^3H]-estrone-3-sulfate (F) for 2 min, respectively, was determined at 37 °C in medium containing in the presence of 5 mM ATP (closed columns) or AMP (open columns). Each point represents the mean \pm S.E. (n = 3). *: p < 0.05; **: p < 0.01

Fig. 3 Time profiles for the transcellular transport of [^3H]-pitavastatin across MDCKII monolayers expressing human transporters. Transcellular transport of [^3H]-pitavastatin (0.1 μM) across MDCKII monolayers expressing OATP1B1 (B), BCRP (C), MDR1 (D), MRP2 (E), both OATP1B1 and BCRP (F), both OATP1B1 and MDR1 (G) and both OATP1B1 and MRP2 (H) was compared with that across the vector-transfected control MDCKII monolayer (A). Open and closed circles represent the transcellular transport in the apical-to-basal and basal-to-apical direction, respectively. Each point represents the mean \pm S.E. (n=3). Where vertical bars are not shown, the S.E. values are within the limits of the symbols.

Fig. 4 Time profiles for the transcellular transport of [^3H]-pitavastatin across MDCKII monolayers expressing rat transporters. Transcellular transport of

[³H]-pitavastatin (0.1 μM) across MDCKII monolayers expressing Oatp1b2 (B), Mrp2 (C), both Oatp1b2 and Mrp2 (D) was compared with that across the vector-transfected control MDCKII monolayer (A). Open and closed circles represent the transcellular transport in the apical-to-basal and basal-to-apical direction, respectively. Each point represents the mean ± S.E. (n=3). Where vertical bars are not shown, the S.E. values are within the limits of the symbols.

Fig. 5 Plasma concentrations and biliary excretion rate of [³H]-pitavastatin during constant intravenous infusion into Sprague-Dawley rats and EHBR. The plasma concentration (A) and biliary excretion rate (B) of total radioactivity were determined during constant intravenous infusion into Sprague-Dawley rats (open circles) and EHBR (closed circles). Each point plotted, with its vertical bar, represents the mean ± S.E. of four rats.

Fig. 6 Plasma concentrations and biliary excretion rate of pitavastatin during constant intravenous infusion into wild type and Bcrp1 (-/-) mice. The plasma concentration (A) and biliary excretion rate (B) of pitavastatin were determined during constant intravenous infusion into wild type (open circles) and Bcrp1 (-/-)

(closed circles) mice. Each point plotted, with its vertical bar, represents the mean \pm S.E. of four mice. *: $p < 0.05$

Table 1 Inhibitory effects of statins on the ATP-dependent uptake of [³H]-estrone-3-sulfate by human BCRP- and mouse Bcrp-membrane vesicles.

Statins	K _i value for hBCRP (μM)		K _i value for mBcrp (μM)	
atorvastatin	14.3	± 1.9	17.6	± 1.7
cerivastatin	18.1	± 2.5	30.1	± 6.3
fluvastatin	5.43	± 0.27	8.62	± 0.86
pitavastatin	2.92	± 0.35	6.00	± 0.71
pravastatin	> 300 μM		> 300 μM	
rosuvastatin	15.4	± 2.4	10.3	± 0.6
simvastatin acid	18.0	± 4.3	24.9	± 3.8

The ATP-dependent uptake of [³H]-estrone-3-sulfate (0.1 μM) for 1 min by human BCRP (hBCRP) and mouse Bcrp (mBcrp) was determined in the presence and absence of unlabeled statins at the designated concentrations. The values are expressed as a percentage of the ATP-dependent uptake of [³H]-estrone-3-sulfate in the absence of any unlabeled compounds. The ATP-dependent uptake was obtained by subtracting the transport velocity in the presence of AMP from that in the presence of ATP. The K_i values were determined by fitting the data using the non-least squares method. The values are expressed as mean ± computer-calculated S.D. (n=3).

Table 2 Pharmacokinetic parameters of pitavastatin during constant intravenous infusion into Sprague-Dawley (SD) rats and EHBR.

	$C_{ss,plasma}$ ng.Eq/mL	CL_{total} mL/min/kg	$CL_{bile,plasma}$ mL/min/kg	$CL_{bile,liver}$ mL/min/kg	Liver Conc. ng.Eq/g	$K_{p,liver}$
SD rat	195 ± 13	6.26 ± 0.49	4.55 ± 0.13	0.248 ± 0.042	4346 ± 406	23.0 ± 3.6
EHBR	179 ± 8	6.75 ± 0.34	5.77 ± 0.53	0.399 ± 0.049	2621 ± 139**	14.7 ± 0.8

Data represent the mean ± S.E (n=4).

$C_{ss,plasma}$: Plasma steady-state concentration (mean of plasma concentration at 210 min)

CL_{total} : Total plasma clearance obtained by dividing the infusion rate by $C_{ss,plasma}$

$CL_{bile,plasma}$: Biliary clearance normalized by the plasma concentration

$CL_{bile,liver}$: Biliary clearance normalized by the liver concentration

$K_{p,liver}$: K_p value obtained by dividing the liver concentration by $C_{ss,plasma}$ (at 210 min)

** : $p < 0.01$

Table 3 Pharmacokinetic parameters of pitavastatin during constant

intravenous infusion into wild type and Bcrp1 (-/-) mice.

	C _{ss,plasma} ng/mL	CL _{total} mL/min/kg	CL _{bile,plasma} mL/min/kg	CL _{bile,liver} mL/min/kg	Liver Conc. ng/g	K _{p,liver}
Wild type	254 ± 21	20.1 ± 1.8	1.21 ± 0.43	0.364 ± 0.032	813 ± 196	3.34 ± 1.03
Bcrp1 (-/-)	213 ± 22	24.2 ± 2.5	0.110 ± 0.02*	0.0293 ± 0.0036**	798 ± 124	3.94 ± 0.83

Data represent the mean ± S.E (n=4). These parameters are explained in

Table 2.

C_{ss,plasma}: Plasma steady-state concentration (mean of plasma concentration at 150 min)

K_{p,liver}: K_p value obtained by dividing the liver concentration by C_{ss,plasma} (at 150 min)

*: p < 0.05; **: p < 0.01

Fig. 1

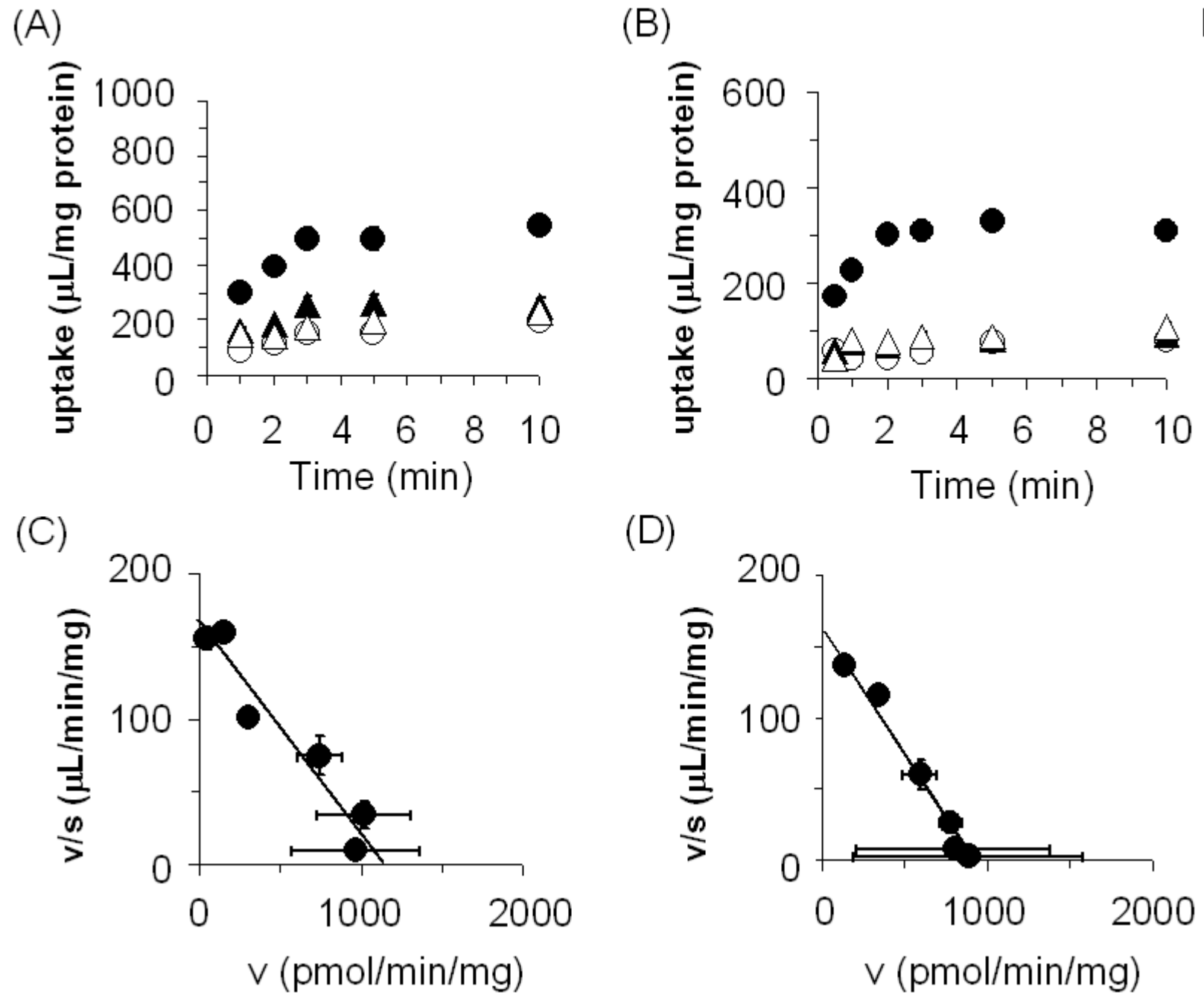


Fig. 2

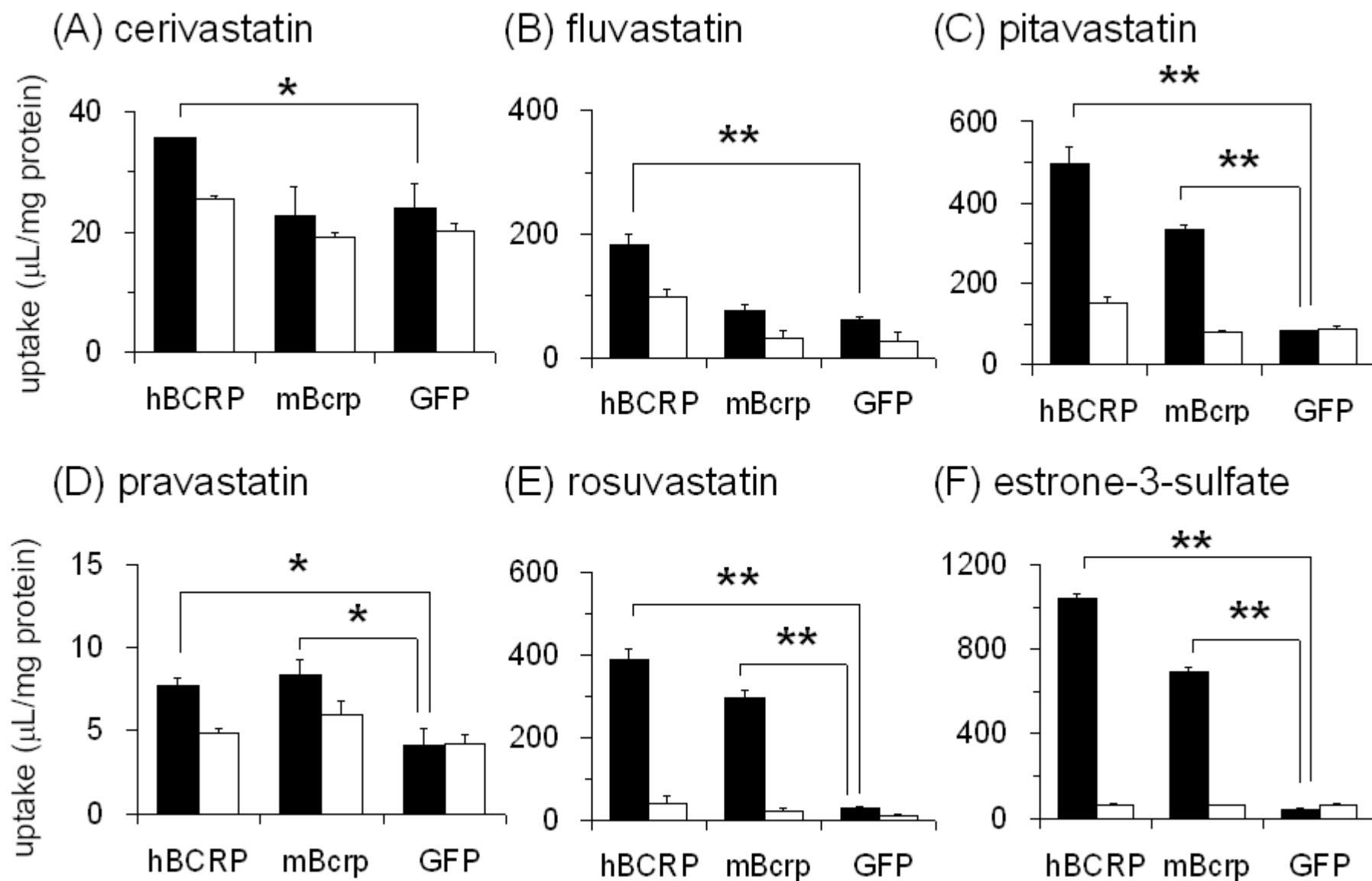


Fig. 3

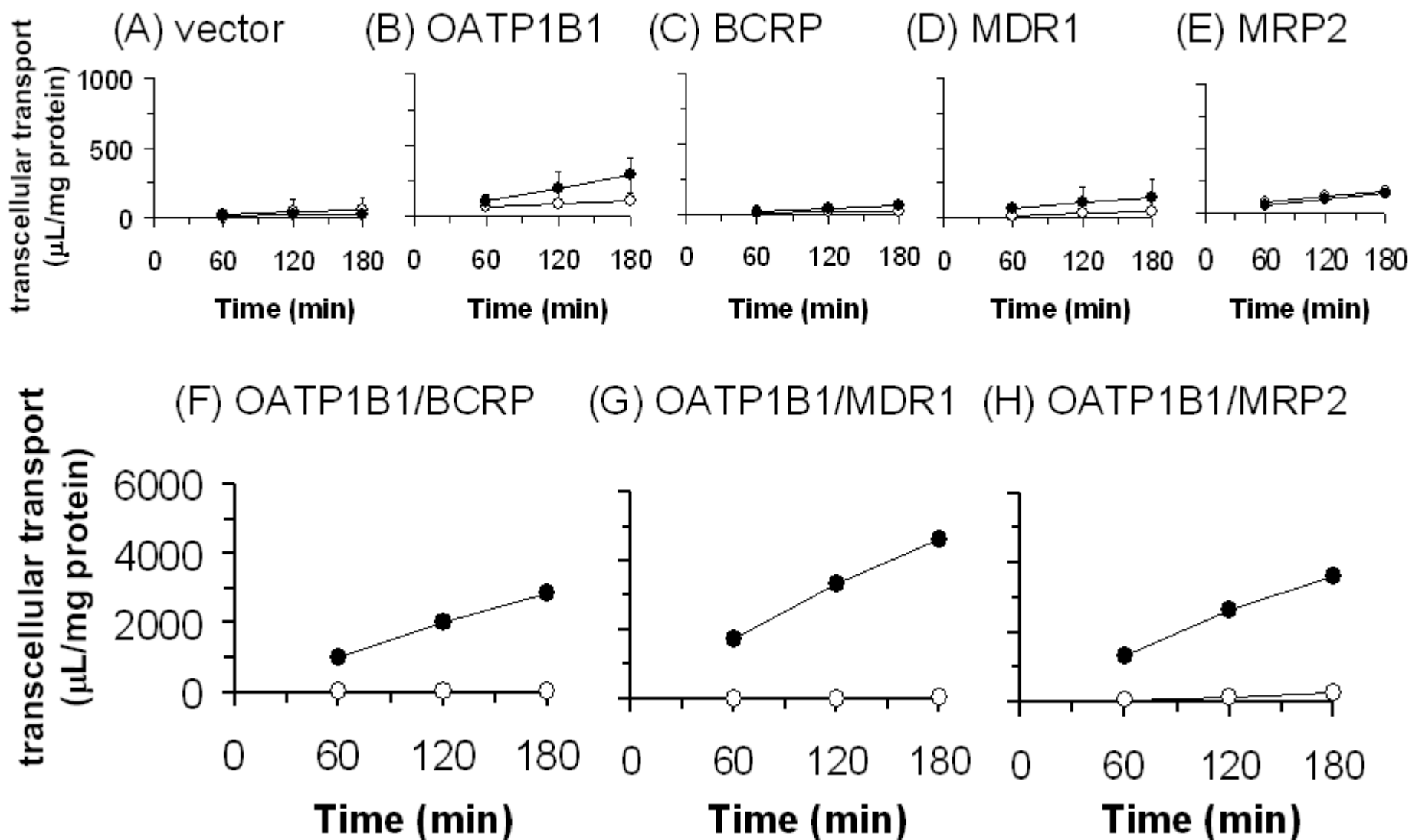


Fig. 4

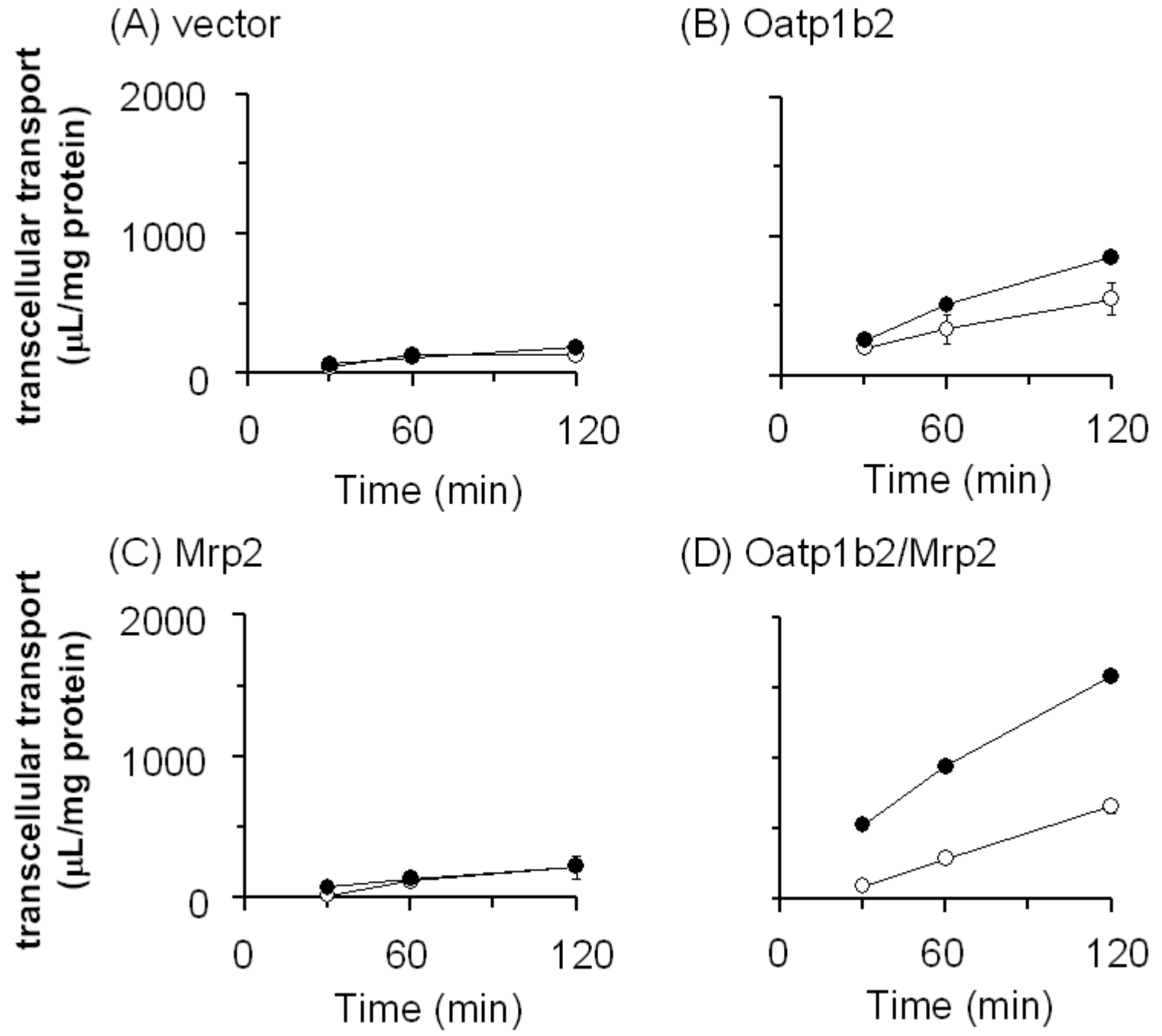


Fig. 5

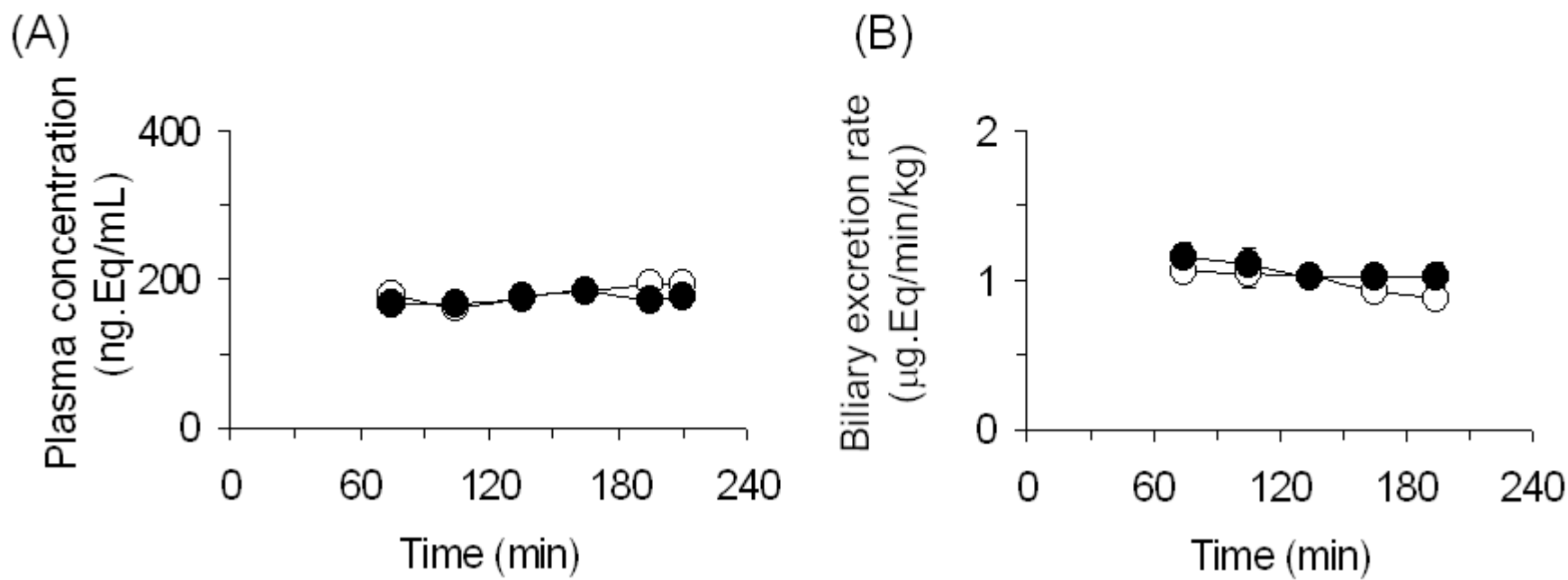


Fig. 6

